Tribology International 73 (2014) 47–56

Contents lists available at ScienceDirect

Tribology International

journal homepage: www.elsevier.com/locate/triboint

Influence of contact stress on rolling contact fatigue of composite ceramic coatings plasma sprayed on a steel roller

Jia-jie Kang [a], Bin-shi Xu [b], Hai-dou Wang [a,b,*], Cheng-biao Wang [a]

[a] School of Engineering and Technology, China University of Geosciences, Beijing 100083, China
[b] National Key Laboratory for Remanufacturing, Academy of Armored Forces Engineering, Beijing 100072, China

ARTICLE INFO

Article history:
Received 5 October 2013
Received in revised form
12 December 2013
Accepted 23 December 2013
Available online 15 January 2014

Keywords:
Rolling contact fatigue
Thermal spray coatings
Failure mechanism

ABSTRACT

The influence of contact stress on rolling contact fatigue performance of plasma sprayed Al_2O_3–40 wt% TiO_2 composite ceramic coating was investigated using a double-roll test machine under pure rolling contact condition. The shear stresses within the coating were analyzed with the three-dimensional finite element method. Three modes of failures, i.e., surface abrasion, spalling, and delamination, were observed during this investigation. The failure mechanisms of surface abrasion, spalling, and delamination were discussed in detail. The initiation and propagation of fatigue cracks were mainly caused by the shear stress, which were highly influenced by the contact stress.

1. Introduction

Ceramic materials have the superior properties of high-temperature resistance, corrosion resistance, wear resistance, high strength, high hardness, and electric insulation [1,2]. Plasma spraying technology with high flame temperature and fast velocity of particles is very suitable for preparing ceramic coatings with high melting point [3–5]. The preparation of ceramic coatings on a metal substrate can combine the high toughness, processability, and thermal conductivity of metal materials with excellent high-temperature resistance, corrosion resistance and wear resistance of ceramic materials to exert the advantages of the two kinds of materials. This can significantly improve the surface properties of mechanical components which are prone to abrasive wear and corrosion wear. Al_2O_3 coating is one of the most widely used ceramic coatings in an industrial equipment. However, Al_2O_3 coatings have the disadvantages of high brittleness and low bonding strength with the metal substrate. Therefore, there are few applications of Al_2O_3 coating to rolling contact machine elements except for some rolls under relatively low contact stress. When a certain amount of TiO_2 is dissolved in Al_2O_3, the toughness, impact resistance of composite ceramic coatings, and the bonding strength between the coatings and the substrate can be improved. Al_2O_3–40 wt% TiO_2 composite ceramic coatings (AT40 coatings) with high content of TiO_2 exhibit relatively high density, toughness, and bonding strength with the substrate. This can greatly improve the rolling contact fatigue (RCF) strength of AT40 coatings.

Many studies on the RCF behavior of thermal spray coatings in rolling contacts have indicated that the performance is dependent on the contact stress during the tests [6,7]. The shear stress within the coating due to the contact stress will remarkably influence the RCF failure mechanism [8,9]. There is an increased demand for RCF behavior, reliability, and load bearing capacity of composite ceramic coating and future applications call for their use in more hostile environments. However, there is few research on the RCF failure mechanism under the effect of contact stress of composite ceramic coatings. In the present study, the RCF behavior and failure mechanism of AT40 coatings under different contact stresses were investigated in detail. As well as an RCF failure model was established based on the simulation of shear stresses within the coating and the analysis of the failed coating specimens.

2. Experimental test procedure

2.1. Coating deposition

A supersonic plasma spray system was used to deposit AT40 composite ceramic coatings and Ni/Al bonding coatings on the surface of a tempered AISI 1045 steel roller with the hardness of 260 $HV_{0.1}$. The micro-morphologies of Ni/Al powders and AT40 composite ceramic powders are shown in Fig. 1. It can be seen that the Ni/Al powders and AT40 powders present sphericity and

* Corresponding author at: School of Engineering and Technology, China University of Geosciences, Beijing 100083, China. Tel.: +86 10 66718475; fax: +86 10 66717144.
E-mail address: wanghaidou@aliyun.com (H.-d. Wang).

0301-679X/$ - see front matter © 2014 Elsevier Ltd. All rights reserved.
http://dx.doi.org/10.1016/j.triboint.2013.12.019

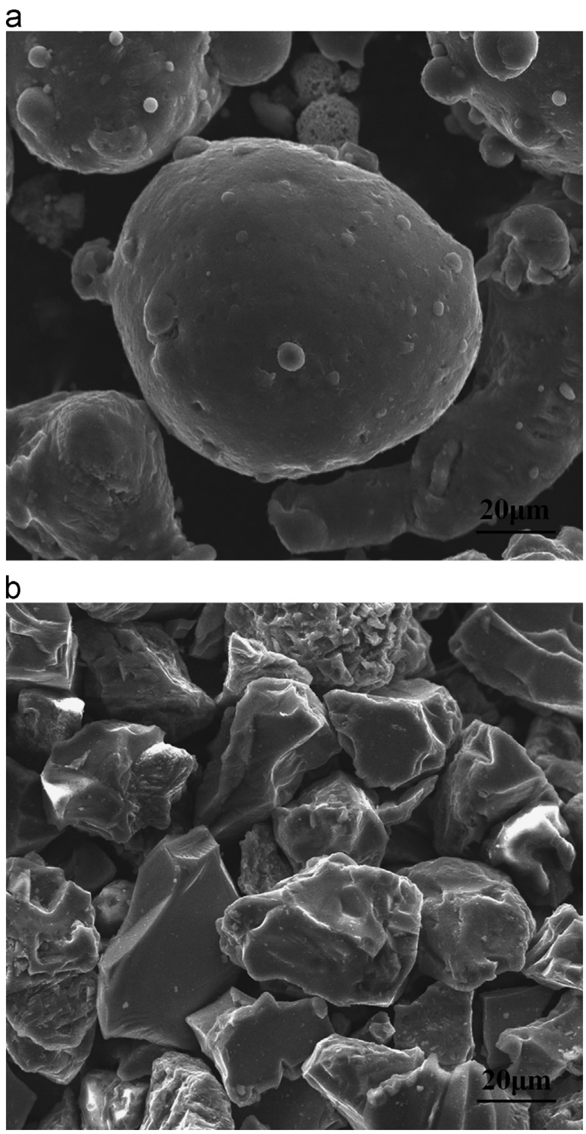

Fig. 1. Micro-morphologies of the spray powders. (a) Ni/Al spray powders and (b) AT40 spray powders.

Table 1
Plasma spraying parameters.

Plasma spray parameters	Spraying materials	
	Ni/Al	AT40
Argon gas flow (m^3/h)	3.4	2.8
Hydrogen gas flow (m^3/h)	0.3	0.4
Nitrogen gas flow (m^3/h)	0.6	0.6
Spraying current (A)	320	440
Spraying voltage (V)	140	110
Spraying distance (mm)	150	100
Powder feed rate (g/min)	30	30

irregular polyhedron, respectively. The plasma spray parameters of depositing the composite ceramic coatings and Ni/Al bonding coatings are presented in Table 1. Prior to the plasma spraying process, the surface of substrate roller was sandblasted and preheated to the temperature of about 200 °C. The average thickness of as-sprayed coating on the test roller was 400 μm. Fig. 2 shows the cross section morphology of the AT40 coating, which presents a relative dense micro-structure with a few micro-defects.

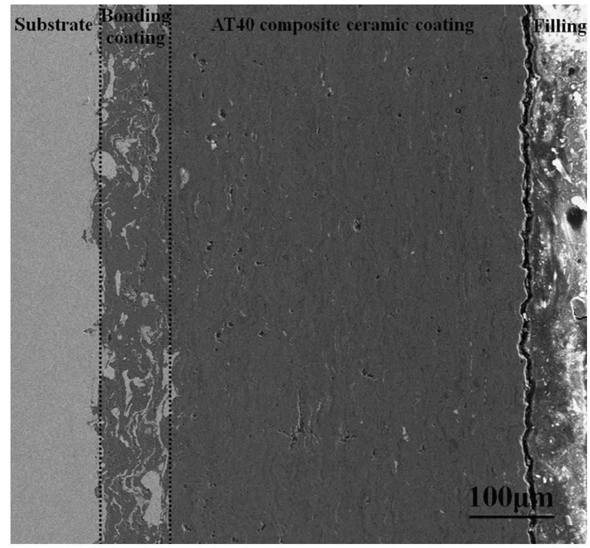

Fig. 2. Cross section morphology of the AT40 coating.

2.2. Experimental conditions and procedures

The rolling contact fatigue (RCF) performance under different contact stress levels was investigated by using a double-roll RCF test machine [10]. The schematic of the test roller and standard roller is shown in Fig. 3(a). The load was applied to the upper roller (test roller) by the hydraulic-lever system. The acoustic emission probe was fixed on the shaft bed to monitor the failure process of the test roller for its sensitivity to plastic deformation and brittle fracture of materials. Only the AE signals over threshold value of 60 dB were collected, as well as the failure point would be judged once the AE count exceeded 350; meanwhile the test machine would stop automatically to keep the original failure morphologies for analyzing. Fig. 3(b) shows the configuration of the test roller and standard roller. AT40 coating was prepared on the external circle surface of the test roller. The length of contact line is 5 mm.

The test rollers were ground to give an average coating thickness and surface roughness of 400 ± 15 μm and 0.62 ± 0.01 μm, respectively. The material of the standard roller was tempered AISI 52100 steel with the hardness of 770 $HV_{0.1}$. The standard rollers were ground to reach the surface roughness of 0.36 ± 0.01 μm. The surface roughness of the test roller and standard roller was measured by an Olympus OLS4000 laser 3D microscope. The micro-hardness, elastic modulus, Poisson's ratio, and surface roughness of the test roller and standard roller are shown in Table 2.

The RCF tests for AT40 coatings were performed under four different contact stresses. The Hertz equation (Eq. (1)) was used to calculate the corresponding loads of four different contact stresses, as presented in Table 3. At least 10 tests were conducted at each contact stress

$$\sigma_{\max} = \sqrt{\frac{F\left(\sum\rho\right)}{\pi L\left(\frac{1-\upsilon_1^2}{E_1}+\frac{1-\upsilon_2^2}{E_2}\right)}} \tag{1}$$

where $\sigma_{\max}$ is the maximum contact stress, F is the load, L is the length of the contact line, υ_1 and E_1 are Poisson's ratio and elastic modulus of the AT40 coating, respectively, υ_2 and E_2 are Poisson's ratio and elastic modulus of the standard roller, respectively, $\sum\rho$ is the sum of principal curvatures of the test roller and standard roller, which can be calculated by

$$\sum\rho = \frac{1}{R_{11}}+\frac{1}{R_{12}}+\frac{1}{R_{21}}+\frac{1}{R_{22}} \tag{2}$$